

THE FUNDAMENTAL PLANE OF FIELD EARLY-TYPE GALAXIES AT $z = 1$ ¹

A. VAN DER WEL,² M. FRANX,² P. G. VAN DOKKUM,³ AND H.-W. RIX⁴

Received 2003 October 3; accepted 2003 December 8; published 2004 January 19

ABSTRACT

We present deep VLT spectra of early-type galaxies at $z \approx 1$ in the Chandra Deep Field–South, from which we derive velocity dispersions. Together with structural parameters from *Hubble Space Telescope* imaging, we can study the fundamental plane for field early-type galaxies at that epoch. We determine accurate mass-to-light ratios (M/L) and colors for four field early-type galaxies in the redshift range $0.96 < z < 1.14$, and two with $0.65 < z < 0.70$. The galaxies were selected by color and morphology, and have generally red colors. Their velocity dispersions show, however, that they have a considerable spread in M/L (by a factor of 3). We find that the colors and directly measured M/L correlate well, demonstrating that the spread in M/L is real and reflects variations in stellar populations. The most massive galaxies have M/L comparable to massive cluster galaxies at similar redshift and therefore have stellar populations that formed at high redshift ($z > 2$). The lower mass galaxies at $z \approx 1$ have a lower average M/L , and one is a genuine “E+A” galaxy. The M/L indicate that their luminosity-weighted ages are a factor of 3 younger at the epoch of observation, because of either a low formation redshift or late bursts of star formation contributing 20%–30% of the mass.

Subject headings: cosmology: observations — galaxies: evolution — galaxies: formation

1. INTRODUCTION

Good understanding of the formation and evolution of early-type galaxies is one of the major challenges for current structure-formation models. Models of hierarchical structure generally predict that field early-type galaxies form relatively late (e.g., Diaferio et al. 2001). One of the prime diagnostics of the formation history of early-type galaxies is the evolution of the M/L as measured from the fundamental plane (FP; Franx 1993). Studies of the evolution of the luminosity function, together with the evolution of M/L , quantify the evolution of the mass function. Previous studies of the evolution of the M/L have produced consistent results for the evolution of massive cluster early-type galaxies: the evolution is slow, consistent with star formation redshifts $z \approx 2$ (e.g., van Dokkum & Stanford 2003).

On the other hand, studies of the evolution of field galaxies have yielded more contradictory results: whereas early studies found slow evolution (e.g., van Dokkum et al. 2001; Treu et al. 2001; Kochanek et al. 2000), more recently, evidence for much faster evolution was found by Treu et al. (2002) and Gebhardt et al. (2003); and yet other authors found that the majority of field early-types evolve slowly, with a relatively small fraction of fast-evolving galaxies (e.g., Rusin et al. 2003; van Dokkum & Ellis 2003; van de Ven, van Dokkum, & Franx 2003; Bell et al. 2003).

These previous measurements suffered from several uncertainties: the signal-to-noise ratios (S/Ns) of the spectra were generally quite low, much lower than usual for nearby studies of the FP (e.g., Faber et al. 1989; Jørgensen et al. 1996). Those studies, based on lensing galaxies, used stellar-velocity dispersions derived from image separations.

In this Letter, we present high-S/N spectra and accurate measurements of the M/L of four field elliptical galaxies with

$z \approx 1$ –1.14 and two at $z \sim 0.7$ in the Chandra Deep Field–South (CDF-S). The S/Ns are comparable to those obtained for nearby galaxies. Together with accurate multiband photometry available for the CDF-S, we have measured the accurate M/L and rest-frame optical colors at $z \sim 1$.

Throughout this Letter we use Vega magnitudes and assume a Λ -dominated cosmology ($[\Omega_M, \Omega_\Lambda] = [0.3, 0.7]$), with a Hubble constant of $H_0 = 70 \text{ km s}^{-1} \text{ Mpc}^{-1}$.

2. SPECTROSCOPY

2.1. Sample Selection and Observations

The galaxies were selected from the COMBO-17 catalog (see Wolf et al. 2003), and imaging was obtained by the Great Observatories Origin Deep Survey⁵ (GOODS; data release ver. 0.5) from the Advanced Camera for Surveys (ACS) on the *Hubble Space Telescope*. We selected compact, regularly shaped galaxies with photometric redshifts higher than 0.8 and $I-z \geq (I-z)_{\text{Sbc}}$, $z < 2.2$. $(I-z)_{\text{Sbc}}$ denotes the color of the Sbc template of Coleman, Wu, & Weedman (1980) at the photometric redshift. This template has $(U-V)_{z=0} = 0.95$. The typical uncertainty in the color is 0.1 mag. Lower priority galaxies were included with either lower redshifts or later types.

The CDF-S was observed in MXU mode with FORS2 on VLT-UT4 during three runs from 2002 September through 2003 February, for a total of 14 hr. The 600 z grism (central wavelength 9010 Å, resolution 5.1 Å or $\sigma_{\text{instr}} = 72 \text{ km s}^{-1}$) was used. During the observations toward the CDF-S the seeing varied between 0".7 and 1".5, with a median seeing of about 1". The sky was clear all the time.

2.2. Velocity Dispersions

It turned out that 10 out of the 11 high-priority objects at $z_{\text{phot}} \sim 1$ have the spectrum of a quiescent galaxy; the other one has a bright [O II] emission line. The brightest four ($z \lesssim 21.0$, independent of the color) had sufficient S/Ns to perform reliable dispersion measurements. The rest-frame spectra of these four galaxies are shown in Figure 1. They all show

¹ Based on observations collected at the European Southern Observatory, Chile (169.A-0458).

² Leiden Observatory, P.O. Box 9513, J. H. Oort Building, Niels Bohrweg 2, NL-2300 RA, Leiden, Netherlands.

³ Department of Astronomy, Yale University, P.O. Box 208101, New Haven, CT 06520-8101.

⁴ Max-Planck-Institut für Astronomie, Königstuhl 17, D-69117 Heidelberg, Germany.

⁵ See <http://www.stsci.edu/science/goods>.

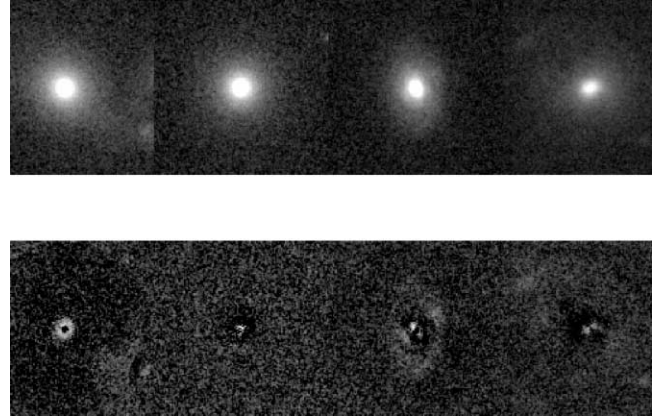
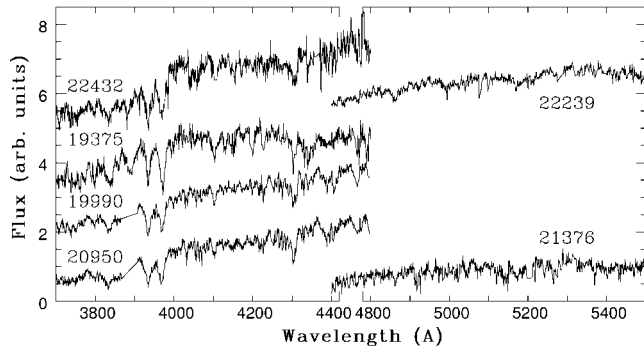


FIG. 1.—*Left*: Unsmoothed rest-frame spectra of the six objects with velocity dispersions. Regions with bright sky lines are interpolated. The wavelength scale is interrupted at $\lambda = 4500$ Å. *Right*: ACS images (F850LP) of the four galaxies at $z \sim 1$, and the residual images from the $r^{1/4}$ fit. *From left to right*: 20950, 19990, 19375, and 22432.

a strong 4000 Å break and Ca lines. Balmer lines (especially the H δ line) are also present, although varying in strength from object to object (see Table 1). Object 19375 is an “E+A” galaxy, according to the criteria used by Fisher et al. (1998). For two ellipticals with $0.65 < z < 0.70$ we also have sufficient signal to determine a velocity dispersion.

Dispersions were measured by convolving a template star spectrum to fit the galaxy spectrum as outlined by van Dokkum & Franx (1996). We tested this procedure extensively, using different template stars and masking various spectral regions. The final values for the velocity dispersions (see Table 1) were obtained by masking the Ca H and K and Balmer lines and using the best-fitting template spectrum, which was a high-resolution solar model spectrum⁶ smoothed and rebinned to match the resolution of the galaxy spectra. The Ca lines were not included in the fit because this greatly reduced the dependence of the measured velocity dispersions on template type. The tests using different templates and different masking of the Ca lines indicate that the systematic uncertainty is $\sim 5\%$.

In order for the results to be comparable to previous studies, an aperture correction as described by Jørgensen, Franx, & Kjørgaard (1995b) was applied to obtain velocity dispersions within a circular aperture with a radius of $1''.7$ at the distance of the Coma Cluster. This correction is $\sim 7\%$.

This is the first extensive sample of such objects at $z > 0.9$ with high S/N (see van Dokkum & Ellis 2003; Treu et al. 2002; Gebhardt et al. 2003, for other spectroscopic studies).

⁶ See <http://bass2000.obspm.fr>.

3. PHOTOMETRY

Photometry and structural parameters were determined from the GOODS ACS images (data release ver. 1.0). Images are available in four filters (F435W, F606W, F775W, and F850LP), which we refer to as b , v , i , and z , respectively.

For each object, the effective radius (r_e) and the surface brightness at the effective radius (μ_e) were obtained by fitting an $r^{1/4}$ profile, convolved by the point-spread function (PSF; van Dokkum & Franx 1996); z -band images were used for the $z \sim 1$ objects, and i -band images for the $z \sim 0.7$ objects. Stars were used as the PSF. The resulting values for r_e and μ_e vary by $\approx 10\%$ when using different stars, but also correlate such that the error is almost parallel to the FP (van Dokkum & Franx 1996). Therefore, the errors in our results are dominated by the errors in the velocity dispersions. The results are listed in Table 1. The images of the $z \sim 1$ objects and the residuals of the fits are shown in Figure 1.

To determine the $i-z$ and $v-i$ colors, fluxes were calculated from the $r^{1/4}$ model within the measured effective radius. To this model flux we added the flux within the same radius in the residual images. We corrected for Galactic extinction based on the extinction maps from Schlegel, Finkbeiner, & Davis (1998). The correction is extremely small: $E(B-V) = 0.007$.

Rest-frame B -band surface brightnesses and rest-frame $U-V$ colors were obtained by transforming observed flux densities in two filters to a rest-frame flux density exactly as outlined by van Dokkum & Franx (1996). The spectral energy distribution used to calculate the transformations is the early-type spectrum from Coleman et al. (1980). We found the same

TABLE 1
PHOTOMETRIC AND SPECTROSCOPIC PROPERTIES

ID	α (arcsec)	δ (arcsec)	z_{spec}	i	$v-i$	$i-z$	$\log r_e$ (kpc)	μ_e	S/N (Å ⁻¹)	σ (km s ⁻¹)	(H γ + H δ)/2 (Å)	[O II] (Å)
19375	0	-50	1.089	21.72	1.71	1.04	-0.410 ± 0.012	21.75 ± 0.05	26	198 ± 25	4.1	-4.6
19990	-32	-35	0.964	21.32	1.89	1.00	-0.388 ± 0.007	21.45 ± 0.03	49	159 ± 14	2.5	>-1
20950	-73	-6	0.964	21.18	2.07	1.07	0.0085 ± 0.026	22.95 ± 0.08	39	261 ± 23	<1	>-1
22432	83	41	1.135	22.38	2.00	1.42	-0.109 ± 0.040	23.35 ± 0.13	21	217 ± 20	<1	-4.4
21376	129	10	0.685	21.46	1.77	0.58	-0.447 ± 0.001	22.16 ± 0.04	27	156 ± 24
22239	236	35	0.660	20.67	1.67	0.50	-0.842 ± 0.002	19.83 ± 0.03	40	177 ± 19

NOTE.—Coordinates are in arcseconds east and north of R.A. = $03^{\text{h}}32^{\text{m}}25^{\text{s}}$, decl. = $-27^{\circ}54'00''$. Errors in the magnitudes and colors are, respectively, 0.03 and 0.05 mag. Effective radii and surface brightnesses (mag arcsec⁻² at r_e) are measured in the z -band for objects 19375, 19990, 20950, and 22432, and in the i -band for objects 21376 and 22239. The listed errors in the velocity dispersions are fitting errors and do not include a 5% systematic error.

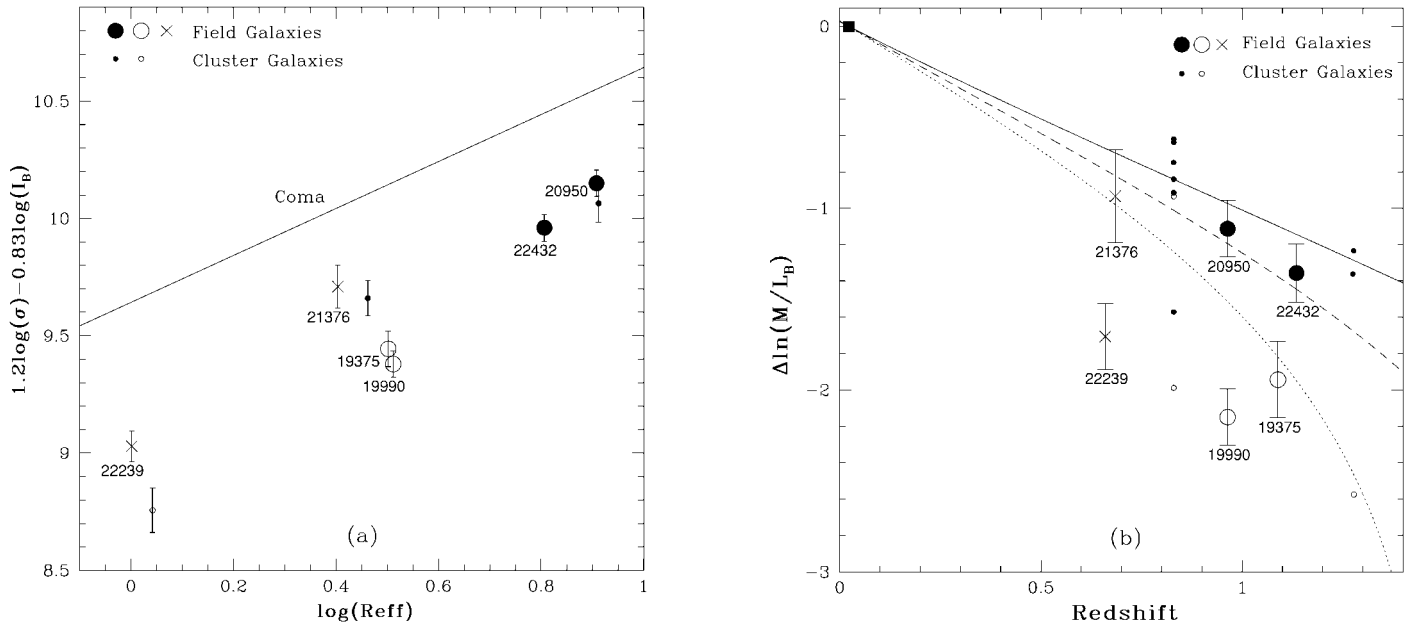


Fig. 2.—(a) FP points of the field galaxies presented in this paper (errors include a 5% systematic effect in the velocity dispersions), the FP points of cluster galaxies at $z = 1.27$ (van Dokkum & Stanford 2003), and the FP of the Coma Cluster (Jørgensen et al. 1996). (b) Offsets in M/L_B from the Coma Cluster FP (square; derived from Jørgensen et al. 1996). Besides the $z = 1.27$ cluster, this figure also contains the data from van Dokkum et al. (1998) on the MS 1054 cluster at $z = 0.83$. The full, dashed and dotted curves are the model predictions for a single burst of star formation with a Salpeter (1955) initial mass function for redshifts 3, 2, and 1.5, respectively. Filled symbols indicate galaxies with masses $M > 3 \times 10^{11} M_\odot$; other symbols indicate galaxies less massive than that. Crosses and squares distinguish between galaxies at $z < 0.8$ and $z > 0.8$, respectively. All galaxies occupying the region below the $z = 1.5$ model curve are “E+A” galaxies, except 19990, and have masses less than $3 \times 10^{11} M_\odot$. The more massive galaxies have significantly older stellar populations.

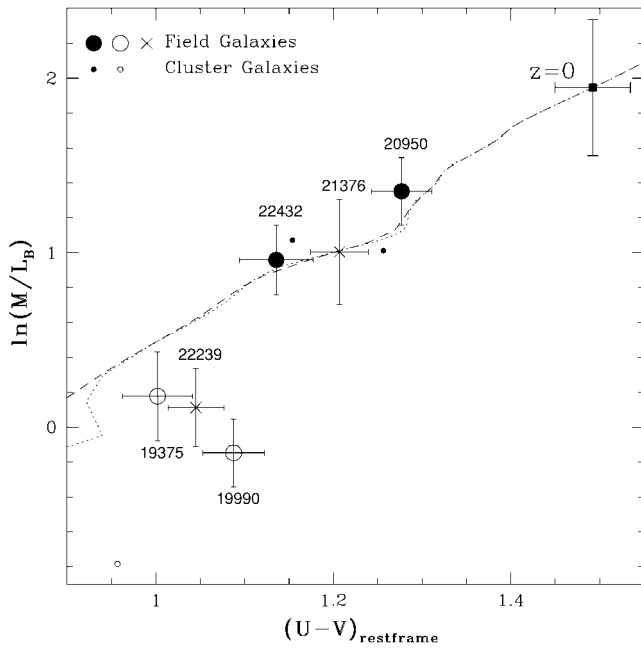


Fig. 3.—Rest-frame $U-V$ color vs. M/L_B in solar units. Filled symbols are objects more massive than $M > 3 \times 10^{11} M_\odot$; open symbols represent the less massive ones. The cluster galaxies are the $z = 1.27$ galaxies from Fig. 2. The redshift zero data point is the average for galaxies with $\sigma > 150 \text{ km s}^{-1}$ in the clusters Abell 194 and DC 2345–28 (Jørgensen, Franx, & Kjærgaard 1995a). The lines are solar-metallicity Bruzual & Charlot (2003) models with constant star formation during the first 200 Myr (dotted line) and exponentially decaying star formation on the same timescale (dashed line).

results for other template spectra. The results are listed in Table 1.

4. MASS-TO-LIGHT RATIOS FROM THE FUNDAMENTAL PLANE

Figure 2a shows the FP for the six field galaxies described above, and the FP for Coma derived by Jørgensen et al. (1996). Additionally, we show the results from van Dokkum & Stanford (2003) on three cluster galaxies at $z = 1.27$. The offsets of the high-redshift galaxies from the Coma FP are a measure of the evolution of M/L . We show the evolution of M/L in Figure 2b as a function of redshift.

Obviously, the field galaxies at $z > 0.6$ span a wide range in offsets, by a factor of approximately 3 in M/L . The error bars on the individual points are much smaller than the offsets. A model with a single-formation redshift can be ruled out at the 99% confidence level, as measured from the χ^2 method. The rest-frame colors of the galaxies confirm the reality of the variations in the M/L . As shown in Figure 3, a very strong correlation exists between the colors and the M/L , in the direction predicted by population synthesis models. The good correlation demonstrates that colors can be used to estimate the M/L , as applied, for example, by Bell et al. (2003), to a large sample of field early-type galaxies.

We note that galaxies in our study lie fairly close to the red sequence and were characterized by Bell et al. (2003) to have red colors. The overall spread in colors of field galaxies is much larger (1.5 mag) compared to the spread found here (0.3 mag).

5. DISCUSSION

On the basis of our high-S/N spectra we have found a rather wide range in M/L for early-type galaxies at $z = 1$, indicating a range in star formation histories. The M/L and colors are well correlated, as expected from stellar population models. Hence, the scatter in M/L is real.

The results agree surprisingly well with earlier results based on lensing galaxies. Rusin et al. (2003) and van de Ven et al. (2003) found a range in M/L , and van de Ven et al. (2003) found a similar correlation between rest-frame colors and M/L . Other authors found either low M/L (e.g., Treu et al. 2002; Gebhardt et al. 2003) or high M/L (e.g., van Dokkum & Ellis 2003), and this is most likely due to (still unexplained) sample selection effects. The last authors found that galaxies with residuals from the $r^{1/4}$ profile had young ages. However, we find no such relation in our sample.

Stellar population models indicate that the low M/L of the blue $z \approx 1$ galaxies may be due to an age difference of a factor of 3. Alternatively, bursts involving 20%–30% of the mass can produce similar offsets. The current sample is too small to determine the fraction of young early-type galaxies at $z \approx 1$ reliably. Large, mass-selected samples are needed for this, as current samples are generally optically selected and therefore biased toward galaxies with lower M/L .

It is striking that the most massive galaxies have modest evolution in M/L , similar to what van Dokkum & Stanford (2003) found for massive cluster galaxies. The evolution of the galaxies with $M = 6.07r_c\sigma^2 \geq 3 \times 10^{11} M_\odot$ (Jørgensen et al. 1996) in our sample is $\Delta \ln(M/L_B) = (-1.17 \pm 0.14)z$. The implied formation redshift is above 2, ignoring the effects of progenitor bias (van Dokkum & Franx 2001). The mass limit is comparable

to the M_* mass of an early-type galaxy: if we take the σ_* of early-type galaxies derived by Kochanek (1994) of 225 km s^{-2} , we derive a typical mass of $M_* = 3.1 \times 10^{11} M_\odot$, based on the sample measured by Faber et al. 1989. The sample as a whole evolves as $\Delta \ln(M/L_B) = (-1.64 \pm 0.45)z$, whereas the sample with masses smaller than $3 \times 10^{11} M_\odot$ evolves as $\Delta \ln(M/L_B) = (-1.95 \pm 0.29)z$.

The results are therefore consistent with little or no (recent) star formation in massive early-type galaxies out to $z = 1$, and younger populations in less massive galaxies, possibly caused by bursts involving up to 30% of the stellar mass. Since these less massive galaxies have much more regular stellar populations at $z < 0.5$ without signs of recent star formation, these results are consistent with the downsizing seen in the field population (Cowie et al. 1996): at progressively higher redshifts, more and more massive galaxies are undergoing strong star formation.

It remains to be seen how this trend continues out to even higher redshifts. The biases inherent in studies of galaxies at $z = 2$ and higher make it very hard to perform similar studies: the optical light has shifted to the near-IR, and spectroscopy is extremely hard at those wavelengths.

More studies at redshift $z \approx 1$ are needed to determine the distribution of colors and M/L of the progenitors of field early-types. Such a determination should be based on mass-selected samples. Further studies of spectral energy distributions extending to the rest-frame infrared will be very useful to better constrain the star formation histories of the bluer galaxies.

We thank the ESO staff for their support during the observations. We thank C. Wolf for making available the COMBO-17 catalog.

REFERENCES

- Bell, E. F., et al. 2003, ApJ, submitted (astro-ph/0303394)
 Bruzual A., G., Charlot, S. 2003, MNRAS, 344, 1000
 Coleman, G. D., Wu, C.-C., Weedman, D. W. 1980, ApJS, 43, 393
 Cowie, L. L., Songaila, A., Hu, E. M., & Cohen, J. G. 1996, AJ, 112, 839
 Diaferio, A., Kauffmann, G., Balogh, M. L., White, S. D. M., Schade, D., & Ellingson, E. 2001, MNRAS, 323, 999
 Faber, S. M., Wegner, G., Burstein, D., Davies, R. L., Dressler, A., Lynden-Bell, D., & Terlevich, R. L. 1989, ApJS, 69, 763
 Fisher, D., Fabricant, D., Franx, M., & van Dokkum, P. 1998, ApJ, 498, 195
 Franx, M. 1993, PASP, 105, 1058
 Gebhardt, K., et al. 2003, ApJ, 597, 239
 Jørgensen, I., Franx, M., & Kjørgaard, P. 1995a, MNRAS, 273, 1079
 ———. 1995b, MNRAS, 276, 1341
 ———. 1996, MNRAS, 280, 167
 Kochanek, C. S. 1994, ApJ, 436, 56
 Kochanek, C. S., et al. 2000, ApJ, 543, 131
 Rusin, D., et al. 2003, ApJ, 587, 143
 Salpeter, E. E. 1955, ApJ, 121, 161
 Schlegel, D. J., Finkbeiner, D. P., & Davis, M. 1998, ApJ, 500, 525
 Treu, T., Stiavelli, M., Bertin, G., Casertano, S., & Møller, P. 2001, MNRAS, 326, 237
 Treu, T., Stiavelli, M., Casertano, S., Møller, P., & Bertin, G. 2002, ApJ, 564, L13
 van de Ven, P. M., van Dokkum, P. G., & Franx, M. 2003, MNRAS, 344, 924
 van Dokkum, P. G., & Ellis, R. S. 2003, ApJ, 592, L53
 van Dokkum, P. G., & Franx, M. 1996, MNRAS, 281, 985
 ———. 2001, ApJ, 553, 90
 van Dokkum, P. G., Franx, M., Kelson, D. D., & Illingworth, G. D. 1998, ApJ, 504, L17
 ———. 2001, ApJ, 553, L39
 van Dokkum, P. G., & Stanford, S. A. 2003, ApJ, 585, 78
 Wolf, C., Meisenheimer, K., Rix, H.-W., Borch, A., Dye, S., & Kleinheinrich, M. 2003 A&A, 401, 73